VIRGINIA JOURNAL OF SCIENCE
OFFICIAL PUBLICATION OF THE VIRGINIA ACADEMY OF SCIENCE

Vol. 61 No. 3 Fall 2010

TABLE OF CONTENTS

Virginia Journal of Science
Volume 61 Number 3
Fall 2010

Foundational Checklist of the Amphibians of Wise County, Virginia

Sarah R.A. Davidson and **David L. Chambers**[1],
Department of Natural Sciences, The University of Virginia's College at Wise, Wise, Virginia 24293, USA.

ABSRTACT

The Appalachian Mountains are arguably home to the highest degree of amphibian diversity in the world, particularly caudate (salamander) biodiversity. Despite the high degree of amphibian endemism in the Appalachians, several regions remain unsurveyed for amphibian species. In addition to this knowledge gap, we are in the midst of alarming amphibian biodiversity loss. Thus, it is of the utmost importance to bridge this knowledge gap by conducting surveys before some of these amphibian species are lost. We surveyed Wise County (previously unsurveyed county in the Appalachian Mountains with no records existing in the primary literature) over two years to assess amphibian species presence. We found 23 different species of amphibians (eight species of frogs and toads; 15 species of salamanders). In addition, we report five new amphibian species occurrences previously unreported in the primary literature within Wise County. However, not all amphibian species expected to occur in Wise County were observed. The primary suspected reason for their lack of occurrence involves habitat loss and/or modification, since the region is heavily exploited for coal and lumber. Overall, our study provides invaluable data in current times of amphibian biodiversity concern as they clarify and expand our knowledge of known amphibian species within the area. Using our work as a foundation, future surveying could assess whether amphibian biodiversity of Wise County are experiencing growth, stability, or decline.

INTRODUCTION

In the wake of accelerated anthropogenic disturbances to nearly every ecosystem on the planet (Walker et al. 2005), population monitoring has never been more critical. Most scientists would argue that we are currently in the wake of the sixth major extinction in Earth's history (Wake and Vredenburg 2008). For example, approximately 33% of all extant amphibian species are facing declining populations (Stuart et al. 2004). Such a dramatic loss of amphibian biodiversity has been linked to several events, including habitat loss and disease (Kiesecker et al. 2001; Mendelson et al. 2006). While the majority of amphibian populations declines appear to be occurring in the tropics (Wake and Vredenburg 2008), amphibian species in the more temperate

[1] To Whom Correspondence Should be Addressed.
Email: chambers@uvawise.edu

regions are not without their vulnerabilities. However, detecting population declines, while being vitally important, is not easily done – particularly in amphibians. Most amphibian populations are constantly in a state of natural flux (Pechmann and Wilbur 1994), and are highly dependent on uncontrollable environmental influences (such as food abundance, climate, and predation). Nevertheless, the preservation and conservation of amphibians is dependent upon population data. Unfortunately, such data are rarely seen in the primary literature; or if they are reported, it is likely because the population has already declined.

Concerning amphibian diversity in temperate North America, the Appalachian Mountains are arguably the most diverse – especially concerning caudate (salamander) diversity. The Appalachians are home to several endemic caudate species (see Lannoo 2005). Because of this high degree of endemism, monitoring populations over time is essential in conservation efforts of these rare and unique species. However, before extensive monitoring programs can be initiated, foundational groundwork concerning the list of native species must be documented. Herein, we report the first list (to the best of our knowledge) of amphibians occurring in Wise County, Virginia in the primary literature. There are, however, works that report the historic distribution of herpetofauna (amphibians and reptiles) in the Commonwealth (see Mitchell and Reay 1999). However, Mitchell and Reay (1999) explicitly state, on several occasions, that extensive fieldwork needs to be conducted in southwest Virginia (including Wise County) to further clarify the unknown distributions of several herpetofaunal species. The goal of this project was to answer this direct call.

METHODS

All amphibian species observations were within Wise County, Virginia (USA) borders during the summer and fall months of 2009, and spring, summer, and fall months of 2010. Wise County is located in southwest Virginia. It is bordered by Pike County, Kentucky (north), Dickenson County, Virginia (northeast), Russell County, Virginia (east), Scott County, Virginia (south), Lee County, Virginia (southwest), Harlan County, Kentucky (west), and Letcher County, Kentucky (northwest). Wise County covers approximately 1050 km^2, including approximately 3 km^2 of water coverage.

Wise County offers truly unique heterogeneous habitats all along elevation gradients since it is situated in the midst of the Appalachian Mountains. These habitats include coniferous, deciduous, and mixed forests and old fields, coupled with urbanized areas. We sought to survey all habitat types that would yield potential amphibian species observations. As a result, careful and thorough reference book and atlas reviews (e.g., Hulse et al. 2001; Lannoo 2005; Mitchell and Reay 1999; Petranka 1998) were conducted in order to identify preferred habitat types of all amphibian species historically known to occur within Wise County. Specifically, we surveyed both public and private land areas (with permission from land owner(s)). However, the vast majority of this study was conducted on public-use land. The bulk of our public-use land surveys were within various regions of the Jefferson National Forest. Indeed, a large potion of Wise County is part of the Jefferson National Forest. Specifically concerning the Jefferson National Forest, we surveyed the following areas and their immediate surroundings: Cave Springs Recreation Area (near Big Stone Gap, Virginia;

including its Loop Trail and numerous adjacent springs), Stone Mountain Trail (near Big Stone Gap, Virginia; including the numerous small streams and small waterfalls adjacent to the trail), High Knob Recreation Area (near Norton, Virginia; including its wooded Day-Use Areas, Lake Trail, Lake Loop Trail, and the numerous adjacent small streams to these trails), Flag Rock Recreation Area (near Norton, Virginia), Guest River Gorge Trail (near Coeburn, Virginia; including the Clinch River and its following branches: Jaybird, Crab Orchard, Pine Orchard, Hurricane, Flat, Lick Log, and Lick), Little Stony Falls (near Coeburn, Virginia; including the small streams along the Little Stony Falls Trail), Red Fox Trail (near Pound, Virginia; including its numerous small streams adjacent to the trail), Pound Lake (near Pound, Virginia; including its numerous small streams flowing in and out of the lake), Cane Patch Recreation Area (near Wise, Virginia; including areas surrounding/in Bad Creek and North Fork Creek), and Phillips Creek Recreation Area (near Wise, Virginia; including Phillips Creek Trail Loop and the numerous small creeks and waterfalls adjacent to the trail). In addition to these public-use localities within the Jefferson National Forest, we surveyed various public-use regions on the approximately 1.6 km^2 campus of the University of Virginia's College at Wise (including its wetlands, three ponds, numerous small streams, and the surrounding wooded area). Opportunistic amphibian species captures, such as chance encounters while driving to and/or from targeted field sites, accounted for a minute portion of our survey.

Most of our amphibian species observations were direct. When surveying terrestrial habitats, we captured amphibians by hand by lifting cover objects (natural cover objects, such as logs and rocks; or unnatural, such as mattresses and tires). The same strategy was employed for surveying most aquatic habitats, with cover objects on stream banks being lifted. However, in some instances, we used dip-nets in aquatic habitats that had a high degree of leaf litter compared to cover object availability along the bank margins. In some instances involving anuran (frog and toad) species, observations were indirect and accomplished by listening for species-specific calls. To further increase our observation success of targeted species, surveys were conducted at various times of the day/night – depending upon the exact ecological niche of each target species. All scientific and standard English names (common names) of each species follow Crother et al. (2000; 2003).

RESULTS

In total, we observed 23 amphibian species in Wise County, Virginia (see Table 1 for complete list). Specifically, we observed eight anuran (frogs and toads) and 15 caudate species. According to Mitchell and Reay (1999), we observed 18 of their 23 (approximately 78%) previously known amphibian species within the county (see Table 1). In addition, we report new occurrences of *Ambystoma maculatum* (Spotted Salamander), *Desmognathus quadramaculatus* (Black-bellied Salamander), *Eurycea l. longicauda* (Long-tailed Salamander), *Hemidactylium scutatum* (Four-toed Salamander), and *Plethodon cinereus* (Red-backed Salamander) within Wise County, Virginia.

TABLE 1: Comparison of all Amphibian Species Known to Occur in Wise County, Virginia.

Amphibian Species	Mitchell and Reay(1999)	This Study
Anura		
Bufo a. americanus (Eastern American Toad)	X	X
B. fowleri (Fowler's Toad)	X	X
Hyla chrysoscelis (Cope's Gray Treefrog)	X	X
Pseudacris brachyphona (Mountain Chorus Frog)	X	
P. c. crucifer (Northern Spring Peeper)	X	X
Rana catesbeiana (American Bullfrog)	X	X
R. clamitans melanota (Northern Green Frog)	X	X
R. palustris (Pickerel Frog)	X	X
R. sylvatica (Wood Frog)	X	X
Caudata		
Ambystoma jeffersonianum (Jefferson Salamander)	X	
A. maculatum (Spotted Salamander)		X*
Aneides aeneus (Green Salamander)	X	
Desmognathus f. fuscus (Northern Dusky Salamander)	X	X
D. monticola (Seal Salamander)	X	X
D. ochrophaeus (Allegheny Mountain Dusky Salamander)	X	X
D. quadramaculatus (Black-bellied Salamander)		X*
D. welteri (Black Mountain Salamander)	X	
Eurycea cirrigera (Southern Two-lined Salamander)	X	X
E. l. longicauda (Long-tailed Salamander)		X*
E. lucifuga (Cave Salamander)	X	X
Gyrinophilus p. porphyriticus (Northern Spring Salamander)	X	X
Hemidactylium scutatum (Four-toed Salamander)		X*
Notophthalmus v. viridescens (Red-spotted Newt)	X	X
Plethodon cinereus (Eastern Red-backed Salamander)		X*
P. glutinosus (Northern Slimy Salamander)	X	X
P. kentucki (Cumberland Plateau Salamander)	X	
P. richmondi (Southern Ravine Salamander)	X	X
Pseudotriton r. ruber (Northern Red Salamander)	X	X

*Denotes new county record for Wise County, Virginia

DISCUSSION

Among the 23 amphibian species documented in this study, we interestingly report the first documented occurrences of *A. maculatum*, *D. quadramaculatus*, *E. l. longicauda*, *H. scutatum*, and *P. cinereus* in Wise County, Virginia (to the best of our knowledge). Though these species have not been reported previously, their occurrence within the county is not altogether surprising. The preferred habitats of mixed

deciduous forests (*A. maculatum* and *P. cinereus*), hardwood or coniferous forests (*H. scutatum*), and mountain stream (*D. quadramaculatus* and *E. l. longicauda*) are all found within Wise County, Virginia borders. In fact, Mitchell and Reay (1999) suspected that *A. maculatum*, *D. quadramaculatus*, and *H. scutatum* could be found once regions in southwest Virginia were properly surveyed. Our study directly answered this survey call.

Mitchell and Reay (1999) report the occurrence of four species that we did not find in our Wise County, Virginia survey. These species include: *Pseudacris brachyphona* (Mountain Chorus Frog), *Aneides aeneus* (Green Salamander), *D. welteri* (Black Mountain Salamander), and *P kentucki* (Cumberland Plateau Salamander). Altogether, the lack of discovery of these species in our study was not surprising. For example, *P. brachyphona* populations across its entire range are in apparent population decline due to deforestation and urbanization (Murdock 1994). Partially because of population decline concerns, the Commonwealth has strict regulations concerning *P. brachyphona* commercialization (Mitchell and Pauley 2005). *Aneides aeneus* is also heavily impacted by anthropogenic disturbances, partially because of its highly specific preferred habitat consisting of rocky outcrops (Pauley and Watson 2005a). While it is not considered a species of concern in the Commonwealth, adjacent states have *A. aeneus* listed as endangered or threatened. *Plethodon kentucki* prefer to occupy pristine, mature hardwood forests. Overexploitation of hardwood resources for commercial products has significantly impacted *P. kentucki* populations across its already small home-range (Pauley and Watson 2005b). Future studies and surveys could attempt to ascertain the population status of these anurans and caudates in Wise County, and southwest Virginia as a whole, since much of the region has herpetological unknowns.

While exceedingly rare in the primary literature, studies such as this survey are vital for amphibian population monitoring efforts. Thus, this study contributes to the herpetofaunal list of Wise County, Virginia, and to the Commonwealth itself, by potentially acting as a foundational baseline of data. However, much more work is needed in future years to monitor Wise County, Virginia amphibians. Population trends can only be established with several years of surveying. Even then, population declines may not obvious (Hairston and Wiley 1993). Nevertheless, these efforts are warranted because of the high degree of amphibian biodiversity and endemism within Wise County, Virginia and the surrounding Appalachian Mountains.

ACKNOWLEDGMENTS

Thanks are due to all the field volunteers for their assistance with various aspects of this project. We also wish to thank the landowners that gave us permission to transverse their private property. Funding for this project was awarded to SRAD by means of an undergraduate student Fellowship in the Natural Sciences at the University of Virginia's College at Wise. All observations were done in compliance with the Institutional Animal Care and Use Committee at the University of Virginia's College at Wise. The authors (SRAD and DLC) contributed equally to this project.

LITERATURE CITED

Hulse, A.C., C.J. McCoy, and E.J. Censky. 2001. Amphibians and Reptiles of Pennsylvania and the Northeast. Cornell University Press. 419 p.

Kiesecker, J.M., A.R. Blaustein, and L.K. Belden. 2001. Complex Causes of Amphibian Population Declines. Nature 410:681-684.

Lannoo, M. 2005. Amphibian Declines: The Conservation Status of United States Species. University of California Press, Berkeley. 1094 p.

Mendelson III, J.R., K.R. Lips, R.W. Gagliardo, G.B. Rabb, J.P. Collins, J.E. Diffendorfer, P. Daszak, R. Ibanez D., K.C. Zippel, D.P. Lawson, K.M. Wright, S.N. Stuart, C. Gascon, H.R. da Silva, P.A. Burrowes, R.L. Joglar, E. La Marca, S. Lotters, L. H. du Preez, C. Weldon, A. Hyatt, J.V. Rodriguez-Mahecha, S. Hunt, H. Robertson, B. Lock, C.J. Raxworthy, D.R. Frost, R.C. Lacy, R.A. Alford, J.A. Campbell, G. Parra-Olea, F. Bolanos, J.J.C. Domingo, T. Halliday, J.B. Murphy, M.H. Wake, L.A. Coloma, S.L. Kuzmin, M.S. Price, K.M. Howell, M. Lau, R. Pethiyagoda, M. Boone, M.J. Lannoo, A.R. Blaustein, A. Dobson, R.A. Griffiths, M.L. Crump, D.B. Wake, and E.D. Brodie, Jr. 2006. Confronting Amphibian Declines and Extinctions. Science 313:48.

Mitchell, J.C., and K.K. Reay. 1999. Atlas of Amphibians and Reptiles in Virginia. Special Publication Number 1. Virginia Department of Game and Inland Fisheries, Richmond, Virginia. 122 p.

Murdock, N.A. 1994. Rare and Endangered Plans and Animals of Southern Appalachian Wetlands. Water, Air and Soil Pollution 77:385-405.

Pechmann, J.H.K., and H.M. Wilbur. 1994. Putting Declining Amphibian Populations in Perspective: Natural Fluctuations and Human Impacts. Herpetologica 50:65-84.

Petranka, J.W. 1998. Salamanders of the United States and Canada. Smithsonian Institution Press. 587 p.

Stuart, S.N., J.S. Chanson, N.A. Cox, B.E. Young, A.S.L. Rodrigues, D.L. Fischman, and R.W. Waller. 2004. Status and Trends of Amphibian Declines and Extinctions Worldwide. Science 306:1783-1786.

Wake, D.B., and V.T. Vredenburg. 2008. Are We in the Midst of the Sixth Mass Extinction? A View from the World of Amphibians. Proceedings of the National Academy of Sciences 105:11466-11473.

Walker, B.G., P.D. Boersma, and J.C. Wingfield. 2005. Field Endocrinology and Conservation Biology. Integrative and Comparative Biology 45:12-18.

Virginia Journal of Science
Volume 61, Number 3
Fall 2010

Modeling and Simulation on Signatures of Mars Minerals

Widad Elmahboub[1], **Edward Yankey**, **Olivia Kerwin**,
Mathematics Department, Hampton University
Hampton VA 23668

ABSTRACT

The objective of this study was to assess the feasibility of identiying minerals on Mars using remotely sensed data. In the process we also investigated the effect of noise of aerosol and dust particles on the spectra of Mars minerals. The remotely sensed data was obtained through modeling and simulation and compared to the lab spectroscopy of the specific minerals in order to make an accurate identification. A linear model was developed using MATLAB Random Number Generator to obtain a simulated image. Part of the information we needed for the linear model was pure pixel information of Mars which was obtained from Mars Spirit images. Random noise was added to the image in order to simulate a real world image. In addition to the random noise, a mathematical model was developed to represent the noise caused by aerosols and dust particles in Mars's atmosphere. The simulation was tested to ensure that it satisfied the appropriate model testing. Our results showed that our linear model was appropriate, and was accepted at a confidence interval of about 95%. The simulated image was then corrected from noise through iterations. The overall accuracy of the corrected image showed an improvement in classification by 25%. The signatures of the spectra of the two images were obtained and compared to the lab spectroscopy of specific minerals. The degradation of noise showed improvement in the spectral analysis of Mars data. The spectral analysis showed the presence of iron oxide, calcium oxide and magnesium oxide leading to the conclusion that the image simulation is reliable in mineral spectral identification.

Key Words
Remote sensing of planetary surface, spectroscopy, and mathematical modeling

INTRODUCTION

Remote Sensing aspect of space science and technology relies mainly on sensors on satellites and mounted in telescopes to monitor Earth, other planetary bodies and distant stars and galaxies. This research is important since extraterrestrial remote sensing may make the greatest contributions to useful knowledge of value to humankind's future. Remote sensing in time became an important means of analyzing the status of what was on the planet's surface: clues as to mineral content (Avery, et.

[1]Contact information: Mathematics Department, Hampton University, 200 Eric Nelson Run, Yorktown VA 23693. E-mail: widad.elmahboub@cox.net.

al., 2001). Mars mineral identification is a growing area in scientific community. Researchers attempted to determine minerals using different approaches. However, mineral identification on Mars is underway through orbital visible-infrared remote sensing in concert with spectroscopic, chemical and magnetic measurements (J. Bishop, 2005). The objective of this research is to determine minerals in Mars in visible and the near-IR (near infrared) (0.35 – 1.4 micrometers) through modeling and simulation and remote sensing techniques as described in the Methods. The objective of this study was to identify minerals on Mars through developing a linear mixture model using remotely sensed data and compared it to the spectroscopy of the specific minerals in order to make an accurate identification . In the process we also investigated the effect of noise of aerosol and dust particles on the spectra of Mars minerals. The applications for this method are numerous, but the most significant would be to remotely determine the mineral make up of a planetary surface accurately.

METHODS

The data were extracted from the Spirit instrument MER-A (Mars Exploration Rover – A, January, 2004). In order to simulate an image composed of a mixture of minerals, end member spectra (EMS) and cover class proportions (CCP) were used.

Principle of Linear Mixture Model

In developing the simulated image, the linear mixture model approach was used. The linear mixture model includes mixtures of nine different classes for three sets of EMS representing minerals with different CCP. The requirement of the linear mixture model depends on the extraction of EMS and the CCP (Jian and Haigh 1997).

To extract the EMS from pure pixel values (X) in a homogenous part of the imagery, a certain number of training sets are predefined and each pixel is assigned to a training set that it resembles. The quality of training sets depends mostly on accuracy of the automated classifier (Lilisand and Kiefer, 1994).

If there are *c* types of ground cover and *n* spectral bands, it is always assumed that $n \geq c$ to avoid the identifiability problem. A column vector $f = [f_1, \ldots . f_c]^T$ is used to denote the proportions of areas within the pixels occupied by each of the c types of ground cover.

In correspondence with the Linear Mixture model, we can formulate the equation below:

$$x_i = \sum M_{\ddot{u}} f_i + e_i \quad , \tag{1}$$

Where $M_{\ddot{u}}$ is independent of f_i and e_i represents noise.

We can rewrite equation (1) in matrix form as:

$$X = mf + e = \mu_1 f_1 + \mu_2 f_2 + \ldots + \mu_c f_c . \tag{2}$$

to estimate $\hat{f}$ which satisfies the constraints such that:

$$\sum_{j-1}^{c} \hat{f}_j = 1, \hat{f}_j > 0, \quad \text{j} = 1,\ldots,\text{c}. \tag{3}$$

In order to ensure that all the error is due to atmospheric noise, the least square method is used. The assumption is that the random noise is confined to E' and denoted as a column vector as $E' = [E_1, \ldots, E2]$ Then equation (2) can be modified to be (Jian and Haigh 1997):

$$X' = \hat{M}F + E' \ . \tag{4}$$

The error can be minimized by using: $\|X' - MF'\|^2$, (Jian, L., and Haigh, J. 1997). Several LS constraining methods were used to estimate the CCP which can be shown in the following.

1. Normalized Least Squares Method

If the estimated $\hat{F}_{LS}$ included a negative element of CCP, they will be set to zero, then the remaining elements will be scaled so that they all total one. For example, when c equals 4 classes, if a vector of the estimated CCP $\hat{F}_{LS}$ is [0.4 -0.05 0.7 -0.06], then the negative proportions -0.05 and -0.06 will first be set to zero, so as to convert to [0.4 0 0.7 0]. Secondly, each proportion will be multiplied by 1 / {sum of elements (0.4+0+0.7+0)} to yield $\hat{F}_{NLS}$ = [4/11 0 7/11 0]. Consequently, this is the closest point to $\hat{F}_{LS}$ while satisfying the constraints of Equation (3), (Settle and Drake, 1994).

2. Lagrangian Least Square Method

Settle and Drake (1994) proposed an algorithm to solve the constrained least squares problem. If the constraints of Equation (3) are satisfied, the new equation can be derived by the Lagrangian analysis, such that

$$\hat{F}_c = \alpha Uj + (1 - Uj)\hat{F}_{LS} \ , \tag{5}$$

Where j = [1,.....,1] ^{T} in a $c \times 1$ matrix where the elements are all 1, $J = jj^T$ is a c × c matrix I in a $c \times c$ identity matrix, U = (M ^{T} M)$^{-1}$ is a $c \times c$ matrix, and α = (JUJ^T)$^{-1}$ is a constant.

Eventually, the newly constrained least squares solution ($\hat{F}_{LLS}$) can be decided such that:

$$\begin{aligned} \hat{F}_{LLS} &= \hat{F}_c && 0 \le j^T \hat{F}_c \le 1 \\ &= (\mathrm{I} - \alpha \mathrm{UJ})\, \hat{F}_c && 0 \ge j^T \hat{F}_c \\ &= \alpha \mathrm{Uj} + (\mathrm{I} - \alpha \mathrm{UJ})\, \hat{F}_c && I \le j^T \hat{F}_c \end{aligned} \tag{6}$$

The solution using the Lagrangian method constraints only the sum to one condition, so the solution may include negative proportions for some elements. Therefore, after finding the solution by using Equation (6), the normalizing method that was discussed in the previous section can be applied for the negative elements.

3. Weighted Least Squares Method

A constraint can be imposed as:

$$C = \left\| \hat{M}F - X \right\|^2 + \lambda^2 \left\| 1 - jF \right\|^2 \tag{7}$$

With a very large weight factor, λ, so that, in a deviation from 1- *j,* F will cause a significant error to C. Consequently, the sum of one condition, $j'F = 1$, is effectively imposed. Equation (7) can be written as the following matrix (Settle and Drake, 1994):

$$C = \left\| \begin{bmatrix} 1 \\ \ldots\ldots 1 \\ \ldots\ldots\ldots 1 \\ \ldots\ldots\ldots\ldots\ldots \lambda^2 \end{bmatrix} \left\{ \begin{bmatrix} \hat{M} \\ 1\ldots\ldots\ldots\ldots 1 \end{bmatrix} \times \begin{bmatrix} f \\ . \\ . \\ f_c \end{bmatrix} - \begin{bmatrix} X_1 \\ . \\ . \\ X_n \\ 1 \end{bmatrix} \right\} \right\|^2 \tag{8}$$

$$C = \left\| \begin{bmatrix} .. \hat{M} \\ \lambda_1 \ldots\ldots\ldots\ldots \lambda_n \end{bmatrix} \times F - \begin{bmatrix} \lambda \\ X \end{bmatrix} \right\|^2 \tag{9}$$

Once the $\hat{M}$ and $\tilde{X}$ minimizing equation (12) are found, then:

$$\hat{F}_{WLS} = \hat{M} + \tilde{X} \tag{10}$$

Where the subscript WLS represents weighted least squares,

$$\hat{M} = \begin{bmatrix} \hat{M} \\ \hline \lambda_1 \ldots\ldots\ldots \lambda_n \end{bmatrix}, \text{ and } \hat{X} = \begin{bmatrix} X \\ \lambda \end{bmatrix}$$

Mathematical Atmospheric Model

The principle of the mathematical atmospheric model is that the light undergoes transformation and nonlinear change as it is scattered by aerosols while passing through the atmosphere. The set of eignvalues represents value of coefficient of the

scattering vector in space. The nonlinear change is proportional to the light intensity (Logan, 2006) as in the following:

$$I'' - \eta I = 0 \tag{11}$$

where $\eta > 0$.
The general solution for the intensity in equation (6) is;

$$I = A\cos \mu x + B \sin \mu x \ , \tag{12}$$

where $\eta = \mu^2$, and its derivative is,

$$I' = -A\mu \sin \mu x - B\mu^2 \cos \mu x \ , \tag{13}$$

$$I'' = -A\mu^2 \cos \mu x - B\mu^2 \sin \mu x \ , \tag{14}$$

Substituting into equation (6), the following matrix is presented:

$$\begin{vmatrix} \cos \mu a - \cos \mu b & \sin \mu a - \sin \mu b \\ \sin u\mu b - \sin \mu a & \cos \mu a - \cos \mu b \end{vmatrix} = 0 \tag{15}$$

We then solve for the eigenvalues;

$$\mu_n = \frac{2n\pi}{b-a} \tag{16}$$

$$\eta_n = \left(\frac{2n\pi}{b-a}\right)^2 \tag{17}$$

The eigenvalue is assumed to be equal to the optical depth in an atmospheric layer as in the following:

$$\eta_n = \frac{K_{sca} \exp(-Z/H) * A * Z}{\cos\theta} \tag{18}$$

where K_{sca} is the scattering coefficient. Z is the altitude in kilometers, and θ, represents the zenith angle (Bohren and Huffman, 1983). This equation can be used for computation of the atmospheric noise that is intercepted by the telescope or the sensor. The atmospheric noise is represented by the following:

$$\delta = \frac{(1 + Area) K_{sca} A * B * Z * T^{pixel}}{(1 + area) K_{sca} A * B * Z + 1} \tag{19}$$

The atmospheric noise will be added to the linear mixture model equation as in the following equation:

$$X' = \hat{M} F + E' + \delta \tag{20}$$

As we mentioned previously this atmospheric noise will be degraded using iteration, trial and error iterations. The accuracy of correction can be measured by the overall accuracy of classification. The corrected image signatures will be compared to the lab spectra of minerals.

Simulation of Linear mixture model

The EMS was obtained by selecting pure pixel values from a perfectly homogenous area of Mars Spirit images, which represent different minerals. Perfectly homogenous areas are designated by similar signatures/spectral values and/or spectrally separable classes as shown by EMS data sets in Table 1. The extracted data set 1 (EMS set 1) consisted entirely of spectrally separable classes with distict signature values (threshold 10 signature values) as shown by band 3 (class1, class 2, and class 3). The EMS data set 2 (EMS set 2) is made up of a mixture of spectrally separable (band 1-class3, band 2-class 3, and band 3-class 3) and similar classes (threshold 6 signature values). The data set 3 (EMS set 3) consisted entirely of spectrally similar classes and do not show any distinct values. We obtained samples of the necessary training sets within the simulated image by using the training set signature editor in ENVI 4.4 (commercial software) where a reference cursor on the screen was used to manually delineate training area polygons in the displayed image. The pixel values within the polygons were used in the software to develop a statistical description file for each training area. The next step is estimate the CCP using the different constraining methods as described previously. Furthermore, to impose the critical constraints, which are the "sum to one" and "make all CCP positive," several methods were used, such as the Normalization, Lagrangian, and Quadratic constraining methods and the weighted constraining method (Settle and Drake, 1994). These methods were tested to determine the best constraining method for this experiment. After deciding upon CCP estimation and constraining methods, evaluations of estimating EMS and its effects on the corresponding CCP estimation were presented in the section above.

The Quadratic Programming method was tested to be the best constraining method as described in linear mixture model. Using the EMS data sets, the pixel values were computed based on Equation (2) using the MATLAB Random Number Generator. The mathematical model was used to derive the atmospheric error. The atmospheric noise errors were added to the EMS to simulate realistic data sets. As mentioned previously, a minimization of the random error in pixel value was implemented (section 2.1). An ASCII file with pixel values was produced and imported in ERDAS IMAGINE as an image file. The image is then corrected for atmospheric noise through trial and error iterations to reduce the atmospheric error and produce enhancement to the classification accuracy. The Maximum Likelihood automated classifier in ENVI (commercial software) was used. At each iteration step, the atmospheric noise was subtracted using initial values of solar zenith angles and scattering coefficient. The iterations were terminated when the overall classification accuracy reached an optimum value. The signature graphs of the corrected image are compared with lab spectra of minerals (Dalton et. al, 2005). The lab spectra of minerals are considered a "fingerprint" (Clark, 1983). If the graph behavior of corrected image signature values is matching the lab spectra of minerals, then we can conclude that the mineral is identified.

RESULTS

Three different EMS data sets or classes with nine subsets were generated in Table 1. After adding the random noise, the CCP was normalized again to make all CCP positive and equal one. The CCP was estimated using the least squares and end member spectra method (LS EMS) with different constraining methods. To avoid an unexpected random effect, we repeated the calculation several times for each noise level. The Roat Mean Square Error (RMSE) of the different combinations of CCP constraining methods by changing the noise level while using the same LS-EMS is shown in Figure 1. The different combinations of CCP constraining methods are L-LS-CCP (Lagrangian-Least Square-Cover Class Proportions), W-LS-CCP (Weighted-Least Squares-Cover Class Proportions, and Q-CCP (Quadratic programming constraining method-cover class proportions).

The different sample sizes may affect the overall results of these experiments. So, the same experiment was performed with changing the sample sizes. The RMSE of different combinations of the CCP estimation and constraining methods by changing the sample sizes while using the same LS-EMS is shown in Figure 2.

The results show that the quadratic programming method proved to be the best constraining method for CCP estimation. This is shown in Figures 1 and 2, indicating that this method performed much better because of a lower (Roat Main Square Error) RMSE, which does not change with sample size. The result was reasonable, because of adding a normally distributed error and testing the sample groups that created the data set.

The simulated image including the atmospheric effect was tested using statistical testing for appropriate model and significant regression model using SAS/STAT software. We presented some selected samples of results which show the regression is significant at 90% confidence interval. Since $F_{k-2,n-k}$ is larger than 14.25 (Milton and Arnold,1986). H_0 is accepted at $p < 0.025$ at 97.5% confidence. Therefore it can be concluded that the model is appropriate.

The simulated image for minerals with atmospheric noise/effects is shown in Figure 3. The corrected simulated image from atmospheric effects is shown in Figure 4. The correction accuracy is presented by the overall accuracies of classification at the final iteration which are shown in Tables 2, 3, 4, 5, 6, and 7. The overall accuracy of classified pixels for the image with atmospheric effect (Figure 3) is 71.42% and for the corrected simulated image (Figure 4) is 97.56%. The overall accuracy shows improvement in classification which ranges between 22% -25 %. The wavelength was plotted versus the spectral signature (spectral radiance) as in Figures 5, 6, and 7.

DISCUSSION AND CONCLUSION

Since the statistical regression test was conducted at 90 % confidence interval for the linear mixture model, we conclude that the regression model is significant. We conclude that the model is appropriate at 97.5 confidence interval. The results of classifications were presented by the error matrices for three minerals as in Tables 2, 3, 4, 5, 6, and 7. In each table, the last row includes the column total represents the truth data. The diagonal and no diagonal elements represeant the classified data The spectral values along the diagonal are higher than the off diagonal ones which indicated

higher accuracy. The overall accuracy showed improvement by 22%-25%. This indicates that the accuracy of correction is significant. We can conclude that the correction using the atmospheric model produced significant classification accuracy. Figures 5, 6, and 7 represent the wavelength versus signatures (spectral radiances) of the simulated image for three minerals that were compared with the experimental spectra of different minerals. The signatures matched the experimental lab spectra for iron oxide, magnesium oxide and calcium oxide. Thus, the spectral analysis showed the presence of iron oxide, calcium oxide and magnesium oxide leading to the conclusion that the image simulation is reliable in mineral spectral identification. The applications for this method are numerous, but the most significant would be to remotely determine the mineral make up of a planetary surface accurately.

LITERATURE CITED

Avery, T.E. and G.L. Berlin. 2001. Fundamentals of Remote Sensing and Air photo Interpretation, 6th Ed., MacMillan Publ. Co., 472 p.

Adams, J.B. 1974. Visible and Near-Infrared Diffuse Reflectance Spectra of Pyroxenes as Applied to Remote Sensing of Solid Objects in the Solar System. Journal of Geophysics Research 79:4829-4836.

Bishop, J.L. 2005. Hydrated Minerals on Mars. Pages 65-96 in Water on Mars and Life (Advances in Astrobiology and Biogeophysics) Tetsuya Tokano ed. Springer-Verlag, Berlin.

Bohren C. and D. Huffman. 1983. Absorption and Scattering of Light by Small Particles, 2nd ed., New York, NY: Wiley Interscience.

Clark, R.N. 1983. Spectral Properties of Mixtures of Montmorillonite and Dark Carbon Grains: Implications for Remote Sensing Minerals Containing Chemically and Physically Adsorbed Water. Journal of Geophys Research 88:10635-10644.

Dalton, J.B, O. Prieto-Ballesteros, J.S. Kargel, C.S. Jamieson, J. Jolivet, and R. Quin. 2005. Spectral Comparison of Heavily Hydrated Salts with Disrupted Terrains on Europa. Elsevier Inc.

Elmahboub, W. 2009. A combined methodology to produce highly accurate classification for AVIRIS hyperspectral data. Canadian Journal of Remote Sensing 35(4):321-335.

Elmaboub, W. M. 2000. An Integrated Atmospheric Correction and Classification System for Remote Sensing Data to Improve Correction and Classification .Accuracy, doctoral diss, University of Wisconsin–Madison, Madison, WI, 250 p.

Jian, L. and J.Haigh. 1997. Simulated Reflectance Technique for ATM Image Enhancement. Remote Sensing18(2):243-254.

Lilesand, T. and R. Kiefer. 1994. Remote Sensing and Image Interpretation 3rd Ed, John Wiley & Sons, New York.

Logan D.J. 2006. Applied mathematics. Second Edition. Wiley Interscience.

Milton, J.S. and J.C. Arnold. 1986. Probability and Statistics in Engineering and Computing Sciences. Mc-Graw-Hill.

Settle, J.J. and N.A. Drake. 1993. Linear Mixing and the Estimation of Ground Cover Proportions. International Journal of Remote Sensing 14(6):1159-1177.

Spiegel, M.R. and L.J. Stephens. 1999. Problems of Statistics. Third Edition. McGraw-Hill.

ACKNOWLEDGMENTS

This work was under the supervision of Dr. W. Elmahboub in the Mathematics Department at Hampton Univeristy. Mr. Yankey assisted in developing the linear mixture model using MATLAB and ENVI 4.4. Ms Kerwin assisted in writing the first draft of this paper.

TABLE 1. EMS set1, 2, and 3

EMS	Sets	Band 1	Band 2	Band 3	Label
EMS set 1	class 1	54	50	67	subset 1
	class 2	58	57	71	subset 2
	class 3	59	55	101	subset 3
EMS set 2	class 1	142	146	150	subset 4
	class 2	148	150	154	subset 5
	class 3	131	131	144	subset 6
EMS set 3	class 1	241	242	246	subset 7
	class 2	245	243	249	subset 8
	class 3	257	250	252	subset 9

TABLE 2 Corrected image of mineral 1. Higher diagonal elements than non diagonal pertain to higher accuracy being achieved with correction compared to Table 3.

Classified Data	Min. 1	Min. 2	Min. 3	Row Total
Min. 1	12	0	0	12
Min. 2	1	19	0	20
Min. 3	0	0	9	9
Column Total (truth data)	13	19	9	41

TABLE 3 Classification of the noisy image of mineral 1. Less diagonal elements and more non diganoal elements compared to Table 2 which pertain to less accuracy.

Classified Data	Min. 1	Min. 2	Min. 3	Row Total
Min. 1	**11**	8	1	20
Min. 2	2	**9**	0	11
Min. 3	0	2	**8**	10
Column Total (truth data)	13	19	10	41

TABLE 4 Classification of corrected image of mineral 2. Higher diagonal elements than non diagonal pertain to higher accuracy being achieved with correction compared to Table 5.

Classified Data	Min. 1	Min. 2	Min. 3	Row Total
Min. 1	**12**	0	0	12
Min. 2	0	**16**	0	16
Min. 3	0	0	**11**	11
Column Total (truth data)	12	16	11	39

TABLE 5 Classification of the noisy image of mineral 2. Less diagonal elements and more non diganoal elements compared to Table 4 which pertain to less accuracy.

Classified Data	Min. 1	Min. 2	Min. 3	Row Total
Min. 1	**7**	5	0	12
Min. 2	5	**11**	0	16
Min. 3	0	0	**11**	11
Column Total (truth Data)	12	16	11	39

TABLE 6 Classification of the noisy image of mineral 3. Higher diagonal elements than non diagonal pertain to higher accuracy being achieved with correction compared to Table 7.

Classified Data	Min. 1	Min. 2	Min. 3	Row Total
Min. 1	**7**	5	0	12
Min. 2	1	**13**	0	14
Min. 3	0	0	**7**	7
Column Total (truth data)	8	18	7	33

TABLE 7 Classification of corrected image of mineral 3. Less diagonal elements and more non diganoal elements compared to Table 6 which pertain to less accuracy.

Classified Data	Min. 1	Min. 2	Min. 3	Row Total
Min. 1	**8**	0	0	8
Min. 2	0	**18**	0	18
Min. 3	0	0	**7**	7
Column Total (truth data)	8	18	7	33

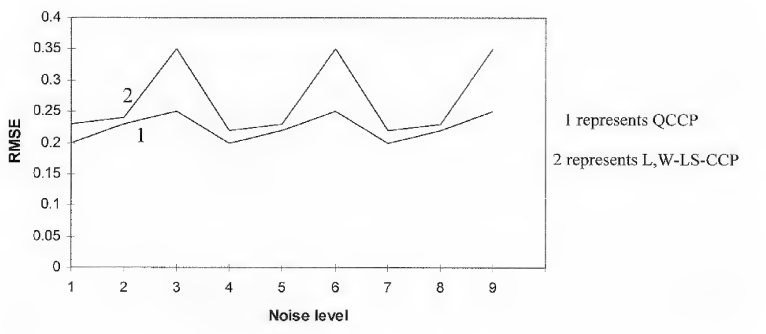

FIGURE 1. RMSE of CCP estimation and constraining methods

.

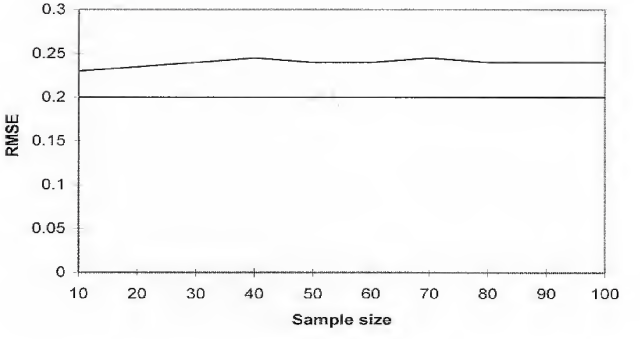

FIGURE 2. RMSE of CCP estimation and constraining methods by changing sample sizes

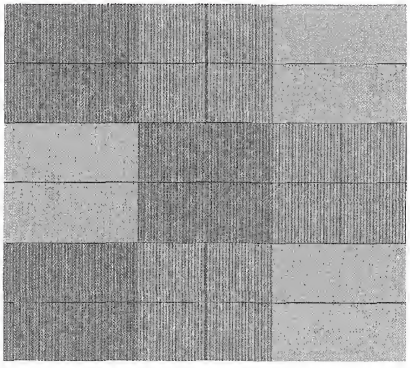

FIGURE 3. The simulated image with atmospheric noise.

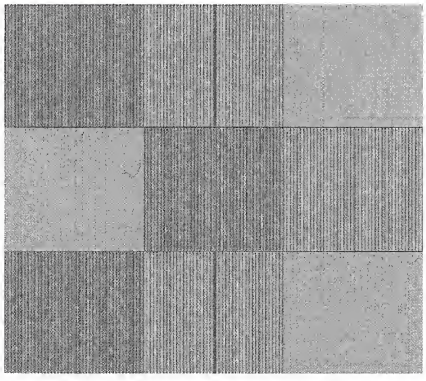

FIGURE 4. Corrected simulated image.

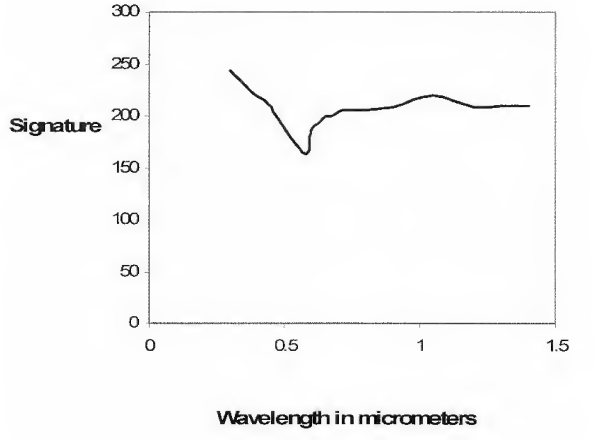

FIGURE 5. Wavelength in micrometer versus signature (in spectral radiance) shows the presence of calcium oxide when compared to lab spectra of USGS.

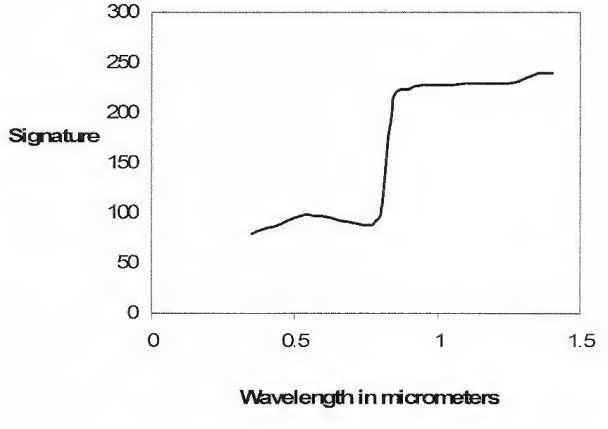

FIGURE 6 Wavelength in micrometers versus signature (in spectral radiance) shows the presence of iron oxide when compared to lab spectra of USGS.

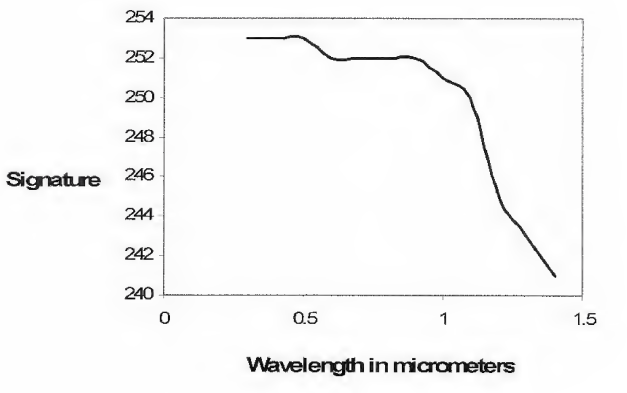

FIGURE 7. Wavelength in micrometer versus signature (in spectral radiance) shows the presence of magnesium oxide when compared to lab spectra (USGS).

THOMAS ORR SITZ (1944-2010)

Past Academy President (1995-1996), Dr. Thomas Orr Sitz, of Blacksburg, Virginia died Tuesday, September 28, 2010 at Montgomery Regional Hospital. Born in Newport, Rhode Island on December 9, 1944 to the late John Harry and Margaret McCullough Sitz. He received a B.S. in Biology from Virginia Tech in 1967 and a Ph.D. in Biochemistry in 1971. Dr. Sitz received a prestigious post-doctoral appointment at Baylor College of Medicine in Houston, Texas under Dr. Harris Busch and was later appointed to a faculty position from 1971-75. He then was a member of the Chemistry Department at Old Dominion University in Norfolk, Virginia where he continued his research from 1975-82. Dr. Sitz recently retired from Virginia Tech and was granted Professor Emeritus. He was Associate Professor of Biochemistry and Anaerobic Microbiology in the College of Agriculture and Life Science, and Director of Premedical Studies. He was the recipient of the Alumni Award for Excellence in Undergraduate Advising in 1982.

He is survived by his wife, Bonnie Crabtree Sitz of Blacksburg; daughter and son-in-law, Molly Sitz Moore and husband Rear Admiral Scott P. Moore of Virginia Beach; sisters, Lucy Aginiga of Chula Vista, California, Margaret Cullifer of Hatteras, North Carolina; brother, John Sitz of Ocracoke, North Carolina; grandchildren, Rachel Laughlin Moore, Sarah Buckley Moore, Thomas Dewey Moore, IV.

Dr. Sitz was a strong supporter and treasured asset to the Academy. He will be greatly missed.

Establishment of Thomas O. Sitz Memorial Student Award

When Thomas O. Sitz died in September, after a long battle with cancer, the Virginia Academy of Science and Virginia Tech lost a wonderful colleague andan inspirational friend. He was Associate Professor of Biochemistry and Anaerobic Microbiology and Director of Premedical Studies at Virginia Tech. He served as President of VAS in 1995-1996, was a Fellow of the Academy, and provided leadership and brought his students to the Chemistry Section for many years. The Council of the Academy proposes to honor Tom by establishing a VAS Student Award in memory of his scientific work, his generous teaching, and his joyous spirit. We hope that Tom's colleagues and friends will feel this is a fitting recognition of what his life and example have meant to all of us. Just as Tom focused his energies on developing the next generation of scientists and science education, so, too, does this award seek to serve that noble purpose. To assist the Academy in funding the Sitz Award, we request that you send your contributions to:

Dr. Arthur Conway, Executive Officer
Virginia Academy of Science
Science Museum of Virginia
2500 West Broad Street
Richmond, Virginia 23220

VIRGINIA ACADEMY OF SCIENCE

APPLICATION FOR MEMBERSHIP

Name (Please Print) _____

Home Phone _(____)_____

Office Phone _(____)_____

E-mail _____

Address _____

City _____ State _____ Zip _____

Institution or Business _____

Position -- Title _____

Interest -- Section No.(s) _____ First no. indicates major interest

Contacted by: _____

Make check payable to Virginia Academy of Science and send to:
Virginia Academy of Science
2500 W. Broad St. , Richmond, VA 23220-2054

Membership in the Academy is organized into sections representing various scientific disciplines as follows:

1. Agriculture, Forestry & Aquaculture
2. Astronomy, Mathematics & Physics
3. Microbiology & Molecular Biology
4. Biology
5. Chemistry
6. Materials Sciences
7. Biomedical & General Engineering
8. Geology
9. Medical Sciences
10. Psychology
11. Education
12. Statistics
13. Aeronautical & Aerospace Sciences
14. Botany
15. Environmental Science
16. Archaeology
17. Computer Science
18. Geography
19. Natural History & Biodiversity

Annual Membership Dues - Please check one. Includes subscription to *Virginia Journal of Science*

Check Your Membership Choice:

☐ Student	$ 10.00	☐ Sustaining - Institution	100.00
☐ Regular - Individual	35.00	☐ Business - Regular	100.00
☐ Contributing- Individual	50.00	☐ Business - Contributing	300.00
☐ Sustaining - Individual	75.00	☐ Business - Sustaining	500.00
☐ Life - Individual	500.00	☐ Patron	1000.00